A NUMERICAL APPROACH TO MARTENSITIC PHASE TRANSFORMATIONS

Thomas Antretter[*], Franz D. Fischer[*], Georges Cailletaud[**]
[*]*Institute of Mechanics, Montanuniversität Leoben, A-8700 Leoben, Austria*
[**]*Centre des Matériaux, Ecole des Mines, B.P.87, F-91003 Evry Cedex, France*

<u>*Summary*</u> Martensitic phase transformations triggered either thermally or mechanically entail a series of peculiar effects on the macro-scale. A thermodynamic criterion deciding upon the formation of a new martensite variant is interpreted as transformation surface bounded by planes, which can be adapted for use as a material subroutine in a finite element program. In combination with flow-plasticity such a concept enables to explain the overall mechanical consequences of transformation induced plasticity.

INTRODUCTION

The present study investigates the peculiarities of MarvalX12, a maraging steel entirely transforming from the austenitic phase into martensite at temperatures low enough to facilitate the experimental verification of the phenomena of interest without having to cope with side effects coming into play in the high temperature regime such as creep. This paper lays out a concept on how to make the thermo-mechanical behavior of materials undergoing a martensitic phase transformation during loading in combination with classical plasticity accessible to a numerical treatment. The relevant equations associated with the phenomenon of transformation induced plasticity have already been derived and presented in [1]. According to this work the issue of transformation is essentially decided by the competition of mechanical and chemical driving forces being a function of the mechanical and thermal state competing with dragging forces represented by the energies required to accommodate the newly created phase.

MODEL

Under certain simplifying circumstances the transformation condition in the notation of [1] can be rewritten in terms of specific quantities as

$$\underline{\sigma} : \underline{\varepsilon}_i^* + \rho \Delta \varphi_{chem}(T) = R_i(\xi_i, \xi_j) . \tag{1}$$

If the equality is satisfied a portion of the parent phase transforms into martensite. The mechanical driving force is defined by the double contraction of the stress state at the start of transformation, denoted by $\underline{\sigma}$ with one of 24 distinct transformation eigenstrains $\underline{\varepsilon}_i^*$ corresponding to each variant known in advance from a crystallographic theory. The chemical driving force $\rho \Delta \varphi_{chem}$ can very well be approximated as a linear function of the temperature T. The right hand side of equation (1) comprises a variety of different mechanisms inhibiting transformation, e.g. a barrier that needs to be overcome in order to rearrange the atoms, a surface energy term and the additional elastic and plastic energies necessary to accommodate the newly created phase. These effects that can be summarized as the dragging forces of martensitic phase transformation are hard to quantify. They essentially depend on the fraction and combination of the martensite variants already present and blocking the space for fitting in a new lath or plate. In this work the symbol ξ_i will be used for the local volume fraction of the *i*-th variant. $R_i(\xi_i, \xi_j)$ represents the function that subsumes the dragging forces. Experimental results involving non-monotonic temperature paths ([2]) give some indication on the shape of this function, and a reasonable fit can be found.

In analogy to the yield locus concept in plasticity martensitic transformation can formally be treated in stress space where the transformation conditions span a surface defining the transformation loci. Each of the 24 equations (1) represents a six-dimensional hyperplane intersecting the neighboring planes, all parameterized by the temperature. Using the terminology of standard plasticity the dragging forces will alternatively be referred to as hardening terms. A small strain setting is assumed for all further relationships. For realistic deformations the resulting error will be small. Then the total strain $\underline{\varepsilon}$ can be decomposed into its various components:

$$\underline{\varepsilon} = \underline{\varepsilon}^{el} + \underline{\varepsilon}^{pl} + \underline{\varepsilon}^{th} + \underline{\varepsilon}^*, \quad \underline{\varepsilon}^* = \sum_{i=1}^{24} \xi_i \underline{\varepsilon}_i^* \tag{2}$$

with $\underline{\varepsilon}^{el}, \underline{\varepsilon}^{pl}, \underline{\varepsilon}^{th}$ being the elastic, plastic and thermal strain in vector notation. The total transformation strain is obtained by adding up the discrete transformation eigenstrains $\underline{\varepsilon}_i^*$ weighted by their respective volume fractions ξ_i. The plastic strain is calculated based on the laws of Mises plasticity, i.e. a yield condition

$$\sqrt{\tfrac{3}{2} \underline{S} : \underline{S}} \le \sigma_y(p) , \tag{3}$$

where $\underline{S}$ denotes the deviator of $\underline{\sigma}$, and $\sigma_y(p)$ is the flow stress as a function of the accumulated plastic strain p thus defining the plastic hardening behavior of the material. For the time being isotropic hardening is assumed. Realistically, only the austenite phase shows non-negligible plastification so the flow rule will be formulated for the austenite only, and the total plastic strain of the composite follows from a rule of mixture, i.e.

$$\dot{\underline{\varepsilon}}_{\gamma}^{pl} = \dot{p}\underline{n}\,, \qquad \underline{\varepsilon}^{pl} = (1 - \sum_{i=1}^{24} \xi_i)\underline{\varepsilon}_{\gamma}^{pl} \tag{4}$$

with $\underline{n}$ being the normal to the yield surface, which can be derived from the flow potential. For the sake of simplicity the influence of the thermal strain will not be discussed here.

For the numerical implementation the relevant equations have to be formulated in an incremental notation. Due to the resulting discretization error the linear strain decomposition, the yield condition and finally the transformation condition are generally violated, so that a vector of residual values $\underline{\Re}_e$, $\Re_p$ and $\Re_t^i$ remains:

$$\underline{\Re}_e = \Delta\underline{\varepsilon}^{el} + (1 - \sum_{i=1}^{24} \xi_i)\Delta p\underline{n} - \sum_{i=1}^{24} \Delta\xi_i\underline{\varepsilon}_{\gamma}^{p} + \sum_{i=1}^{24} \Delta\xi_i\underline{\varepsilon}_i^{*} - \Delta\underline{\varepsilon} \tag{5}$$

$$\Re_p = \sqrt{\tfrac{3}{2}(\underline{S} + \Delta\underline{S}) : (\underline{S} + \Delta\underline{S})} - \sigma_y(p + \Delta p) \tag{6}$$

$$\Re_t^i = (\underline{\sigma} + \Delta\underline{\sigma}) : \underline{\varepsilon}_i^{*} + k(T - T_{ref}) - R(\xi_i + \Delta\xi_i, \xi_j + \Delta\xi_j)\,, \; i, j = 1,...,24 \tag{7}$$

Note that here an implicit formulation has been chosen for the equations (5), (6) and (7) where all state variables are evaluated at the end of the current time increment. Obviously the parameters have to be determined such that the residuals disappear. Then the equations represent a set of 31 non-linear functions of altogether 31 solution variables $\Delta\underline{\varepsilon}^{el}$, Δp and $\Delta\xi_i$. Numerically, this can be accomplished using a root finding algorithm such as the standard Newton-Raphson technique. Note that several constraints on the volume fractions of the variants have to be observed, e.g. the increment of the fraction of each variant must always be positive while the total volume fraction must not exceed 1.

RESULTS

The calculations have been performed at one single material point, subjected to an external stress state. Two different load cases have been investigated with the main focus on the orientation effect, i.e. the issue which set of variants is selected by a given stress field. Figure 1b shows the evolution of the volume fractions of the active variants for the case of uniaxial tension of 50 MPa as the temperature is decreased below martensite start. It turns out that for this load level only two variants are activated by the selection mechanism which, in turn, favors those variants that create the highest mechanical driving force. In contrast, if the load is reduced to 20 MPa, two additional variants (number 1 and 12) appear, see Figure 1a. Variant 10 is still dominating, but its fraction reaches only about 50%, which is far less than in the case of the higher load. The algorithm yields qualitatively reasonable results in the sense that the number of active variants increases as the load level decreases.
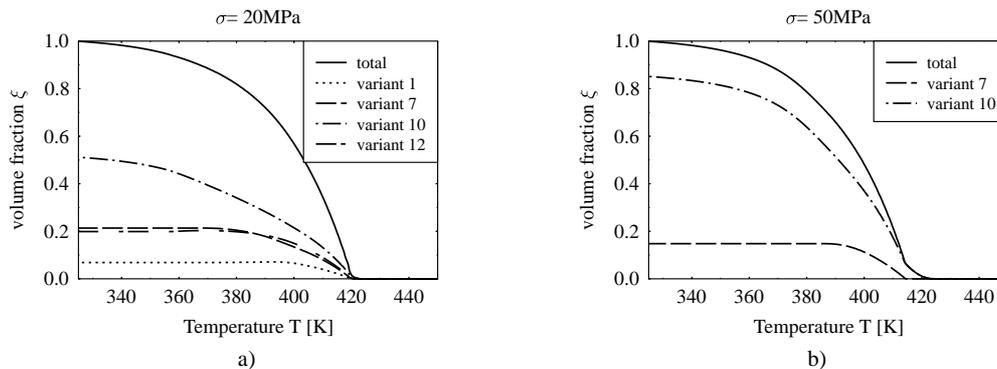

Figure 3: Variant evolution for two different load levels: a) 20 MPa, b) 50MPa.

CONCLUSIONS

An equivalent formalism as for classical flow plasticity establishes the theoretical foundation of the numerical scheme presented towards the end of this paper. The presented concept is based on the underlying idea of a transformation surface. The relevant equations for transformation induced plasticity, essentially the strain decomposition, the yield condition and the transformation condition are formulated in an incremental notation and resolved by means of an implicit integration method. Even for uniaxial stress states constant in time, the algorithm finds sets of martensitic variants whose number varies depending on the stress level. For higher loads one of the active variants prevails accounting for a significant orientation effect in terms of the overall elongation of the specimen.

References

[1] Fischer, F.D., Reisner, G.: *Acta mater.* **46**:2095-2102, 1998.
[2] Tanaka, K., Terasaki, T., Goto, S., Antretter, T., Fischer, F.D., Cailletaud, G.: *Mater. Sci. Eng.* **A341**:189-196, 2002.